J Biomol NMR (2012) 54:9–14
DOI 10.1007/s10858-012-9656-z

COMMUNICATION

Conformational exchange of aromatic side chains characterized by L-optimized TROSY-selected ^{13}C CPMG relaxation dispersion

Ulrich Weininger · Michal Respondek · Mikael Akke

Received: 7 May 2012 / Accepted: 12 July 2012 / Published online: 26 July 2012

Abstract Protein dynamics on the millisecond time scale commonly reflect conformational transitions between distinct functional states. NMR relaxation dispersion experiments have provided important insights into biologically relevant dynamics with site-specific resolution, primarily targeting the protein backbone and methyl-bearing side chains. Aromatic side chains represent attractive probes of protein dynamics because they are over-represented in protein binding interfaces, play critical roles in enzyme catalysis, and form an important part of the core. Here we introduce a method to characterize millisecond conformational exchange of aromatic side chains in selectively ^{13}C labeled proteins by means of longitudinal- and transverse-relaxation optimized CPMG relaxation dispersion. By monitoring ^{13}C relaxation in a spin-state selective manner, significant sensitivity enhancement can be achieved in terms of both signal intensity and the relative exchange contribution to transverse relaxation. Further signal enhancement results from optimizing the longitudinal relaxation recovery of the covalently attached ^{1}H spins. We validated the L-TROSY-CPMG experiment by measuring fast folding–unfolding kinetics of the small protein CspB under native conditions. The determined unfolding rate matches perfectly with previous results from stopped-flow kinetics. The CPMG-derived chemical shift differences between the folded and unfolded states are in excellent agreement with those obtained by urea-dependent chemical shift analysis. The present method enables characterization of conformational exchange involving aromatic side chains and should serve as a valuable complement to methods developed for other types of protein side chains.

Keywords Relaxation dispersion · Conformational exchange · Protein folding · Aromatic side chain · TROSY

Conformational transitions are intimately tied to protein function. Numerous reports have shown that transiently populated high-energy states play important roles in enzyme catalysis (Cole and Loria 2002; Eisenmesser et al. 2002; Sprangers et al. 2005; Boehr et al. 2006) or ligand binding by conformational selection (Malmendal et al. 1999; Brüschweiler et al. 2009). Intermittent transitions between different conformations generally lead to modulation of NMR parameters, such as the chemical shift (Gutowsky and Saika 1953) or residual dipolar couplings (Igumenova et al. 2007; Vallurupalli et al. 2007), resulting in exchange contributions to transverse relaxation rates. Biologically relevant exchange correlation times often fall in the range of milliseconds, which can be probed by NMR relaxation dispersion methods, such as the $R_{1\rho}$ (Akke and Palmer 1996) or Carr-Purcell-Meiboom-Gill (CPMG) experiment (Carr and Purcell 1954; Meiboom and Gill 1958) and variants thereof (Loria et al. 1999a, b; Igumenova and Palmer 2006). These experiments provide a powerful means of characterizing exchange processes in terms of the exchange rate, k_{ex}, the relative populations of the exchanging states, p_i, and the difference in chemical shift, $\Delta\omega$, or residual dipolar coupling between them. In addition to the applications mentioned above, relaxation dispersion methods have proven very successful in

Electronic supplementary material The online version of this article (doi:10.1007/s10858-012-9656-z) contains supplementary material, which is available to authorized users.

U. Weininger · M. Respondek · M. Akke (✉)
Department of Biophysical Chemistry, Center for Molecular Protein Science, Lund University, P.O. Box 124, 22100 Lund, Sweden
e-mail: mikael.akke@bpc.lu.se

studying protein folding, including characterization of transition states as well as intermediate states (Grey et al. 2006; Neudecker et al. 2006; Teilum et al. 2006b; O'Connell et al. 2009; Korzhnev et al. 2010). To date, experiments have been designed to probe conformational exchange at specific sites in proteins, including the backbone (Akke and Palmer 1996; Loria et al. 1999a, b; Hill et al. 2000; Mulder and Akke 2003; Lundström and Akke 2005a, b; Igumenova and Palmer 2006; Lundström et al. 2008, 2009a) and side-chain aliphatic (Lundström et al. 2009b; Hansen et al. 2012), carbonyl/carboxyl (Paquin et al. 2008; Hansen and Kay 2011), and methyl groups (Mulder et al. 2002; Brath et al. 2006; Baldwin et al. 2010; Otten et al. 2010).

Aromatic residues are prevalent in protein binding interfaces, where they contribute significantly to the binding free energy (Bogan and Thorn 1998; Lo Conte et al. 1999; Birtalan et al. 2010). His and Tyr also play prominent roles in enzyme catalysis (Bartlett et al. 2002). Furthermore, aromatic side chains make up a significant proportion of the protein interior, and therefore provide an attractive means of probing the dynamics of the hydrophobic core in the native state (Wüthrich and Wagner 1975), as well as the formation of the core in protein folding reactions. Thus, there is great incentive to extend the existing repertoire of CPMG-type experiments to probe also aromatic side chains in proteins.

We have previously introduced a method for fractional (50 %), site-specific ^{13}C labeling of proteins using 1-$^{13}C_1$-glucose or 2-$^{13}C_1$-glucose, which produces samples with isolated ^{13}C spins thereby eliminating unwanted relaxation pathways and coherent magnetization transfer via one-bond couplings (Teilum et al. 2006a; Lundström et al. 2007). Here, we present a sensitivity-enhanced CPMG relaxation experiment for measuring millisecond conformational exchange of aromatic side chains in selectively ^{13}C labeled proteins, based on longitudinal- and transverse-relaxation optimized spectroscopy, denoted L-TROSY (Pervushin et al. 1998; Loria et al. 1999b; Pervushin et al. 2002; Eletsky et al. 2005; Weininger et al. 2012). Figure 1 outlines the pulse sequence for the L-TROSY-CMPG relaxation dispersion experiment for aromatic ^{13}C spins.

We applied the L-TROSY-CPMG experiment to characterize fast folding–unfolding of cold-shock protein B (CspB) from *Bacillus subtilis* (Schindler et al. 1995) under native conditions. CspB was expressed in *Escherichia coli* cultured on medium containing 1-$^{13}C_1$-glucose as the sole carbon source, resulting in enrichment of ^{13}C into the δ positions of Phe, δ1 and ε3 of Trp, and δ2 and ε1 of His. CspB contains 7 Phe, 1 Trp, 1 His, but no Tyr.

Figure 2 shows the relaxation dispersion curves acquired using the L-TROSY-CPMG experiment for ^{13}C-labeled aromatic side chains. As observed from the comparison with the corresponding data obtained using a regular (i.e. non-L-TROSY) relaxation-compensated (rc) CPMG experiment (Loria et al. 1999a), TROSY-selection achieves significant reduction of the natural linewidth, resulting in increased precision of the measured transverse relaxation rates and vastly improved dynamic range of the relaxation dispersion; see inset of Fig. 2a and Fig. S1. The TROSY effect is expected to be optimal at static magnetic field strengths of approximately 14–15 T, as calculated based on the chemical shielding anisotropy of benzene (Veeman 1984). At 11.7 T, the transverse relaxation rate of the TROSY line is approximately 30 % of the transverse ^{13}C autorelaxation rate. TROSY is expected to provide sensitivity enhancement for larger proteins with a rotational correlation time of $\tau_c \geq 13$ ns (Weininger et al. 2012). CspB has $\tau_c = 4.4$ ns at 25 °C, implying that in this case TROSY does not provide any sensitivity enhancement in and of itself. However, longitudinal relaxation optimization (Pervushin et al. 2002; Eletsky et al. 2005; Weininger et al. 2012) offers significant sensitivity enhancement per unit time, already for a small protein like CspB. In particular, ^{13}C sites located nearby ^{1}H spins that exchange with solvent, e.g. δ1 of Trp or δ2 and ε1 of His, reach gains in signal-to-noise of up to 50 % in the case of CspB. This enhancement is greater than that (10–35 %) documented previously for the larger protein Gal3C (Diehl et al. 2010; Weininger et al. 2012), presumably due to the greater extent of solvent exposure of the aromatic residues in CspB compared to Gal3C. Sensitivity enhancement by L-optimization is expected to increase progressively with molecular weight and static magnetic field strength. As previously described in detail, careful control of the water and aliphatic magnetizations is required in order to obtain accurate relaxation data and optimal sensitivity enhancement using L-optimized experiments (Weininger et al. 2012). In the pulse sequence presented here (Fig. 1), water and aliphatic ^{1}H magnetizations are aligned along $+z$ during the CPMG, t_1 evolution, and acquisition periods.

Significant dispersion profiles were obtained for 9 out of 11 aromatic residues in CspB. The data are adequately represented by a global two-state (folded/unfolded) model using the Carver-Richards equation (Carver and Richards 1972; Palmer et al. 2001), with $k_{ex} = 528 \pm 52$ s^{-1} and a population of the unfolded state of $p_U = 2.3 \pm 0.2$ % (Fig. 2a–d). By contrast, the relaxation data obtained using the rc-CPMG sequence (Fig. 2a, inset; Fig. S1) suffer severely from the fast transverse relaxation of the averaged ^{13}C doublet (roughly a factor of two greater than that of the spin-state selective TROSY line), and are clearly not of sufficient quality to warrant further interpretation.

In the context of the L-TROSY-CPMG experiment, it is critical to recognize that the decay of antiphase coherences (e.g. 2CyHz) can be affected by strong coupling between

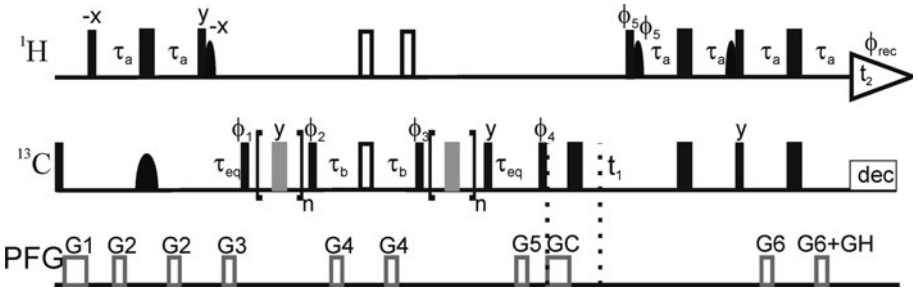

Fig. 1 Pulse sequence of the L-TROSY-CPMG relaxation dispersion experiment for measuring conformational exchange of aromatic side chains in specifically ^{13}C labeled proteins. All pulses are applied along the x-axis unless otherwise indicated. *Narrow (wide) solid bars* indicate rectangular high-power 90° (180°) pulses. *Wide open bars* indicate composite 180° pulses. *Wide grey bars* indicate 180° pulses in the CPMG elements, which have attenuated power (by 6 dB). *Solid semi-ellipses* represent shaped pulses. *Narrow semi-ellipses* on ^{1}H are 90° EBURP2 shapes (Geen and Freeman 1991) centered at 1.9 ppm with a bandwidth of 6.6 ppm. The wide semi-ellipse on ^{13}C represents a 180° REBURP pulse (Geen and Freeman 1991) with a bandwidth of 40 ppm. ^{13}C is decoupled during acquisition using GARP (Shaka et al. 1985). The delays τ_a, τ_b and τ_{eq} are set to 1.5, 1.4 and 5 ms, respectively. The pulses flanking the CPMG blocks purge non-refocused magnetization remaining as a consequence of the variation among aromatic sites in the $^1J_{HC}$ coupling constant (Vallurupalli et al. 2007). The magnetizations from water and aliphatic ^{1}H spins are aligned along the +z axis whenever possible, including the CPMG blocks. The phase cycle is: $\phi_1 = 4(x), 4(-x)$, $\phi_2 = (y, -y)$, $\phi_3 = (x, -x)$, $\phi_4 = (y, x, -y, -x)$, $\phi_5 = (-y)$, $\phi_{rec} = (x, -y, -x, y, -x, y, x, -y)$. Pulsed field gradients G1–6 are employed to suppress unwanted coherences and artifacts, while GC and GH are encoding and decoding gradients, respectively, for echo/anti-echo coherence selection, obtained by inverting the signs of ϕ_5, GC and the even-numbered phases of the receiver (Palmer et al. 1991; Kay et al. 1992). Gradient durations (in ms) and power levels (G/cm) are set to (duration, power level): G1 = (1.0, 10); G2 = (0.5, 8); G3 = (0.5, 14); G4 = (0.5, 16); G5 = (0.5, –24); G6 = (0.5, 18); GC = (1.0, 54); GH (0.5, 27.018). For every second t_1 increment, ϕ_4 and the receiver were incremented

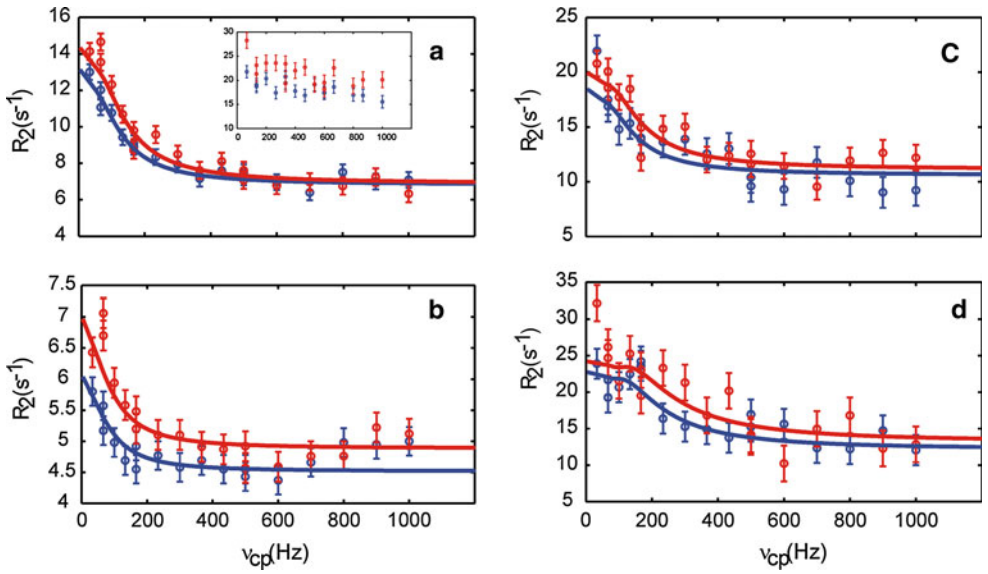

Fig. 2 Representative ^{13}C aromatic L-TROSY-CPMG relaxation dispersion profiles acquired on a 0.4 mM sample of CspB in 10 mM HEPES pH 7.0 at 25 °C and static magnetic field strengths of 11.7 T (*blue*) and 14.1 T (*red*). Data are shown for residues F15δ* (a), F38δ* (b), W8δ1 (c) and H29ε1 (d). The inset in *panel a* shows the corresponding data acquired with the rc-CPMG sequence. The solid lines in (a–d) represent global fits of the folding–unfolding model to the experimental data. Relaxation delays where chosen so as to get the same signal decay (about 50 %) in all experiments, resulting in delays of 60 ms (L-TROSY-CPMG) or 30 ms (rc-CPMG). Supplementary Information Figure S1 shows results for all residues, including rc-CPMG data and L-anti-TROSY-CPMG data

the ^{1}H spin covalently attached to the monitored ^{13}C spin and neighboring ^{1}H spins, which makes the effective R_2 rates depend on the refocusing frequency ν_{cp} also in the absence of conformational exchange (van Ingen et al. 2009). In the case of aromatic spin systems, such aberrant dispersions can become significant if strong scalar coupling occurs between vicinal ^{1}H spins (e.g. ^{1}Hδ1 and ^{1}Hε1 in Phe) for which $^3J_{HH} \approx 8$ Hz, whereas weaker coupling constants (e.g. $^4J_{HH} \approx 2$ Hz, across the ring) do not cause any significant problems irrespective of the frequency difference between the coupled ^{1}H spins, in agreement with previous results (van Ingen et al. 2009). His δ2 and ε1 and

Trp $\delta 1$ ^{1}H spins are always weakly coupled to their vicinal ^{1}H neighbors, which are covalently attached to nitrogen and therefore resonate far downfield. In the case of Phe and Tyr residues, rapid ring flipping makes it impossible to determine a priori whether the weak coupling limit applies. However, numerical simulations using QSim (Helgstrand and Allard 2004) demonstrate that artifactual dispersion decays caused by strong scalar coupling level out completely for $\nu_{cp} \geq 100$ Hz, where the ^{13}C–^{1}H scalar interaction is effectively decoupled. Furthermore, the artifactual dispersion magnitudes are generally limited to $R_2(\nu_{cp} = 0) - R_2(\nu_{cp} \rightarrow \infty) \leq 3\ s^{-1}$. These two criteria serve as useful guidelines for establishing the accuracy of relaxation dispersions measured for Phe and Tyr.

In CspB, H29ε1 and W8δ1 both show dispersion steps of approximately 10 s^{-1} (Fig. 2c–d). Two out of seven Phe exhibit dispersions of 4–6 s^{-1} (as exemplified by F15δ, Fig. 2a), which also can be safely attributed to conformational exchange. Three remaining Phe rings show smaller dispersion steps of 2 s^{-1} (as exemplified by F38δ, Fig. 2b), and 2 rings do not show any appreciable relaxation dispersion. All aromatic ^{13}C dispersion curves of CspB reach a plateau at $\nu_{cp} > 200$ Hz, clearly indicating that the dispersions arise from conformational exchange, rather than from effects of strong coupling. Thus, we conclude that the present data are unhampered by any strong coupling between protons and accurately reflect exchange between folded and unfolded states.

The unfolding rate, $k_U = 12 \pm 3\ s^{-1}$ (derived from the fitted parameters: $k_U = k_{ex} \cdot p_U$) matches perfectly with that ($12 \pm 7\ s^{-1}$) determined previously from stopped-flow data (Schindler et al. 1995), whereas the folding rates differ by a factor of two. Notably, it has been observed for CspB that k_U is almost independent of urea concentration, whereas the folding rate (k_F) exhibits a strong urea dependence (Schindler et al. 1995), indicating that the former is considerably more robust with respect to variations in solvent conditions, such as the difference in buffer composition between the present (10 mM HEPES) and previous (20 or 100 mM sodium cacodylate; Schindler et al. 1995; Zeeb and Balbach 2005) experiments. At the level of individual ^{13}C sites, no deviations from two-state folding behavior were observed, in agreement with previous results (Schindler et al. 1995; Zeeb and Balbach 2005). In the present case, ring flips are expected to be significantly faster than the folding–unfolding kinetics. Consequently, the two processes are time-scale separated, such that CPMG dispersion measurements report only on the folding–unfolding process, while exchange due to ring flips in CspB is too fast to be probed by current refocusing rates.

We assessed the accuracy of the chemical shift differences between the folded and unfolded states determined from the CPMG dispersions by comparing with shift differences measured from ^{1}H–^{13}C HSQC spectra of the folded and unfolded states. ^{13}C chemical shifts of the unfolded state under native conditions were obtained by monitoring the urea-dependence of the ^{1}H–^{13}C HSQC spectrum from 0.5 to 2.5 M urea and extrapolating linearly to 0 M (Fig. S2). Residue-specific assignments of Phe ^{13}Cδ resonances in the unfolded state were not necessary, because they all merged to a single overlapped signal.

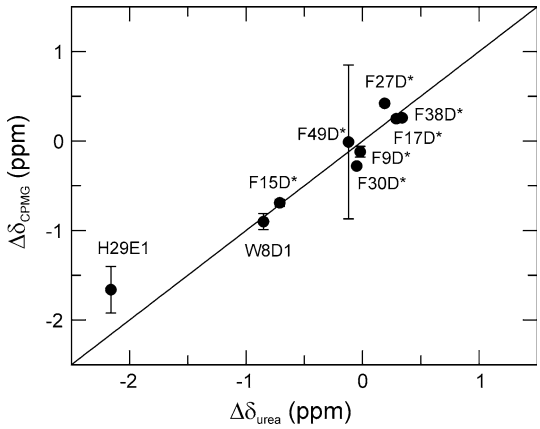

Fig. 3 Correlation of ^{13}C chemical shift differences, $\Delta\delta = \Delta\omega/(2\pi\gamma B_0)$, between the folded and unfolded states of CspB derived from L-TROSY-CPMG relaxation dispersions under native conditions or measured directly from ^{1}H–^{13}C HSQC spectra of the native and progressively urea-denatured states. The signs of the shift differences measured from spectra were also used for the CPMG-derived shift difference. Standard errors of the fitted parameters (vertical axis) were determined from the covariance matrix, whereas the uncertainties of the HSQC-derived shift differences are negligibly small. Sizeable uncertainties are observed only for F49δ*, which has a chemical shift difference close to zero, and H29ε1, which has low signal intensity (Fig. S1); for other residues the error bars are smaller than, or similar to, the size of the symbols

Figure 3 shows the excellent agreement of the chemical shift differences extracted from the global fit to the CPMG dispersion data, compared to the shift differences between the folded and unfolded states derived from ^{1}H–^{13}C HSQC spectra. These results demonstrate that aromatic ^{13}C chemical shift differences between ground (e.g. folded) and high-energy (e.g. unfolded) states can be determined robustly from CPMG dispersion experiments, similar to what has been reported previously for other types of nuclei (Teilum et al. 2006b; Hansen et al. 2008).

In conclusion, the L-TROSY-CPMG relaxation dispersion experiment for aromatic ^{13}C spins provides accurate information on conformational exchange, including the aromatic chemical shifts of the transiently populated high-energy state, and should serve as a valuable complement to experiments developed for other types of side chains.

Acknowledgments We thank Prof. Jochen Balbach for kindly providing the CspB clone. This research was supported by the Swedish Research Council (621-2010-4912; 822-2005-2915), the

Göran Gustafsson Foundation for Research in Natural Sciences and Medicine, and the Knut and Alice Wallenberg Foundation. U.W. was supported by an EMBO long-term fellowship. M.R. was supported by a postdoctoral fellowship funded by the Swedish Research Council (623-2009-800).

References

Akke M, Palmer AG (1996) Monitoring macromolecular motions on microsecond–millisecond time scales by $R_{1\rho}$–R_1 constant-relaxation-time NMR spectroscopy. J Am Chem Soc 118:911–912

Baldwin AJ, Religa TL, Hansen DF, Bouvignies G, Kay LE (2010) $^{13}CHD_2$ methyl group probes of millisecond time scale exchange in proteins by ^1H relaxation dispersion: an application to proteasome gating residue dynamics. J Am Chem Soc 132:10992–10995

Bartlett GJ, Porter CT, Borkakoti N, Thornton JM (2002) Analysis of catalytic residues in enzyme active sites. J Mol Biol 324: 105–121

Birtalan S, Fisher RD, Sidhu SS (2010) The functional capacity of the natural amino acids for molecular recognition. Mol Bio Syst 6:1186–1194

Boehr DD, McElheny D, Dyson HJ, Wright PE (2006) The dynamic energy landscape of dihydrofolate reductase catalysis. Science 313:1638–1642

Bogan AA, Thorn KS (1998) Anatomy of hot spots in protein interfaces. J Mol Biol 280:1–9

Brath U, Akke M, Yang D, Kay LE, Mulder FAA (2006) Functional dynamics of human FKBP12 revealed by methyl 13C rotating frame relaxation dispersion NMR spectroscopy. J Am Chem Soc 128:5718–5727

Brüschweiler S, Schanda P, Kloiber K, Brutscher B, Kontaxis G, Konrat R, Tollinger M (2009) Direct observation of the dynamic process underlying allosteric signal transmission. J Am Chem Soc 131:3063–3068

Carr HY, Purcell EM (1954) Effects of diffusion on free precession in nuclear magnetic resonance experiments. Phys Rev 94:630–638

Carver JP, Richards RE (1972) A general two-site solution for the chemical exchange produced dependence of T_2 upon the carr-purcell pulse separation. J Magn Reson 6:89–105

Cole R, Loria JP (2002) Evidence for flexibility in the function of ribonuclease A. Biochemistry 41:6072–6081

Diehl C, Engström O, Delaine T, Håkansson M, Genheden S, Modig K, Leffler H, Ryde U, Nilsson UJ, Akke M (2010) Protein flexibility and conformational entropy in ligand design targeting the carbohydrate recognition domain of galectin-3. J Am Chem Soc 132:14577–14589

Eisenmesser EZ, Bosco DA, Akke M, Kern D (2002) Enzyme dynamics during catalysis. Science 295:1520–1523

Eletsky A, Atreya HS, Liu GH, Szyperski T (2005) Probing structure and functional dynamics of (large) proteins with aromatic rings: L-GFT-TROSY (4, 3)D HCCHNMR spectroscopy. J Am Chem Soc 127:14578–14579

Geen H, Freeman R (1991) Band-selective radiofrequency pulses. J Magn Reson 93:93–141

Grey MJ, Tang YF, Alexov E, McKnight CJ, Raleigh DP, Palmer AG (2006) Characterizing a partially folded intermediate of the villin headpiece domain under non-denaturing conditions: contribution of His41 to the pH-dependent stability of the N-terminal subdomain. J Mol Biol 355:1078–1094

Gutowsky HS, Saika A (1953) Dissociation, chemical exchange, and the proton magnetic resonance in some aqueous electrolytes. J Chem Phys 21:1688–1694

Hansen AL, Kay LE (2011) Quantifying millisecond time-scale exchange in proteins by CPMG relaxation dispersion NMR spectroscopy of side-chain carbonyl groups. J Biomol NMR 50:347–355

Hansen DF, Vallurupalli P, Lundström P, Neudecker P, Kay LE (2008) Probing chemical shifts of invisible states of proteins with relaxation dispersion NMR spectroscopy: how well can we do? J Am Chem Soc 130:2667–2675

Hansen AL, Lundström P, Velyvis A, Kay LE (2012) Quantifying millisecond exchange dynamics in proteins by cpmg relaxation dispersion NMR using side-chain H-1 probes. J Am Chem Soc 134:3178–3189

Helgstrand M, Allard P (2004) QSim, a program for NMR simulations. J Biomol NMR 30:71–80

Hill RB, Bracken C, DeGrado WF, Palmer AG (2000) Molecular motions and protein folding: characterization of the backbone dynamics and folding equilibrium of alpha D-2 using C-13 NMR spin relaxation. J Am Chem Soc 122:11610–11619

Igumenova TI, Palmer AG (2006) Off-resonance TROSY-selected $R_{1\rho}$ experiment with improved sensitivity for medium—and high-molecular-weight proteins. J Am Chem Soc 128:8110–8111

Igumenova TI, Brath U, Akke M, Palmer AG (2007) Characterization of chemical exchange using residual dipolar coupling. J Am Chem Soc 129:13396–13397

Kay LE, Keifer P, Saarinen T (1992) Pure absorption gradient enhanced heteronuclear single quantum correlation spectroscopy with improved sensitivity. J Am Chem Soc 114:10663–10665

Korzhnev DM, Religa TL, Banachewicz W, Fersht AR, Kay LE (2010) A transient and low-populated protein-folding intermediate at atomic resolution. Science 329:1312–1316

Lo Conte L, Chothia C, Janin J (1999) The atomic structure of protein–protein recognition sites. J Mol Biol 285:2177–2198

Loria JP, Rance M, Palmer AG (1999a) A relaxation-compensated Carr-Purcell-Meiboom-Gill sequence for characterizing chemical exchange by NMR spectroscopy. J Am Chem Soc 121: 2331–2332

Loria JP, Rance M, Palmer AG (1999b) A TROSY CPMG sequence for characterizing chemical exchange in large proteins. J Biomol NMR 15:151–155

Lundström P, Akke M (2005a) Microsecond protein dynamics measured by rotating-frame $^{13}C^a$ spin relaxation. Chem Bio Chem 6:1685–1692

Lundström P, Akke M (2005b) Off-resonance rotating-frame amide proton spin relaxation experiments measuring microsecond chemical exchange in proteins. J Biomol NMR 32:163–173

Lundström P, Hansen DF, Kay LE (2008) Measurement of carbonyl chemical shifts of excited protein states by relaxation dispersion NMR spectroscopy: comparison between uniformly and selectively ^{13}C labeled samples. J Biomol NMR 42:35–47

Lundström P, Hansen DF, Vallurupalli P, Kay LE (2009a) Accurate measurement of alpha proton chemical shifts of excited protein states by relaxation dispersion NMR spectroscopy. J Am Chem Soc 131:1915–1926

Lundström P, Lin H, Kay LE (2009b) Measuring $^{13}C_\beta$ chemical shifts of invisible excited states in proteins by relaxation dispersion NMR spectroscopy. J Biomol NMR 44:139–155

Lundström P, Teilum K, Carstensen T, Bezsonova I, Wiesner S, Hansen F, Religa TL, Akke M, Kay LE (2007) Fractional 13C enrichment of isolated carbons using [1–13C]- or [2–13C]-

glucose facilitates the accurate measurement of dynamics at backbone C^{α} and side-chain methyl positions in proteins. J Biomol NMR 38:122–199

Malmendal A, Evenäs J, Forsén S, Akke M (1999) Structural dynamics in the C-terminal domain of calmodulin at low calcium levels. J Mol Biol 293:883–899

Meiboom S, Gill D (1958) Modified spin-echo method for measuring nuclear spin relaxation times. Rev Sci Instrum 29:688–691

Mulder FAA, Akke M (2003) Carbonyl 13C transverse relaxation measurements to sample protein backbone dynamics. Magn Reson Chem 41:853–865

Mulder FAA, Hon B, Mittermaier A, Dahlquist FW, Kay LE (2002) Slow internal dynamics in proteins: application of NMR relaxation dispersion spectroscopy to methyl groups in a cavity mutant of T4 lysozyme. J Am Chem Soc 124:1443–1451

Neudecker P, Zarrine-Afsar A, Choy WY, Muhandiram DR, Davidson AR, Kay LE (2006) Identification of a collapsed intermediate with non-native long-range interactions on the folding pathway of a pair of Fyn SH3 domain mutants by NMR relaxation dispersion spectroscopy. J Mol Biol 363:958–976

O'Connell NE, Grey MJ, Tang YF, Kosuri P, Miloushev VZ, Raleigh DP, Palmer AG (2009) Partially folded equilibrium intermediate of the villin headpiece HP67 defined by ^{13}C relaxation dispersion. J Biomol NMR 45:85–98

Otten R, Villali J, Kern D, Mulder FAA (2010) Probing microsecond time scale dynamics in proteins by methyl ^{1}H Carr-Purcell-Meiboom-Gill relaxation dispersion NMR measurements. Application to activation of the signaling protein $NtrC^{r}$. J Am Chem Soc 132:17004–17014

Palmer AG, Cavanagh J, Wright PE, Rance M (1991) Sensitivity improvement in proton-detected two-dimensional heteronuclear correlation NMR spectroscopy. J Magn Reson 93:151–170

Palmer AG, Kroenke CD, Loria JP (2001) Nuclear magnetic resonance methods for quantifying microsecond-to-millisecond motions in biological macromolecules. Meth Enz 339:204–238

Paquin R, Ferrage F, Mulder FAA, Akke M, Bodenhausen G (2008) Multiple-timescale dynamics of side-chain carboxyl and carbonyl groups in proteins by C-13 nuclear spin relaxation. J Am Chem Soc 130:15805

Pervushin K, Riek R, Wider G, Wüthrich K (1998) Transverse relaxation-optimized spectroscopy (TROSY) for NMR studies of aromatic spin systems in ^{13}C-labeled proteins. J Am Chem Soc 120:6394–6400

Pervushin K, Vögeli B, Eletsky A (2002) Longitudinal H-1 relaxation optimization in TROSY NMR spectroscopy. J Am Chem Soc 124:12898–12902

Schindler T, Herrler M, Marahiel MA, Schmid FX (1995) Extremely rapid protein-folding in the absence of intermediates. Nat Struct Biol 2:663–673

Shaka AJ, Barker PB, Freeman R (1985) Computer-optimized decoupling scheme for wideband applications and low-level operation. J Magn Reson 64:547–552

Sprangers R, Gribun A, Hwang PM, Houry WA, Kay LE (2005) Quantitative NMR spectroscopy of supramolecular complexes: dynamic side pores in ClpP are important for product release. Proc Natl Acad Sci USA 102:16678–16683

Teilum K, Brath U, Lundström P, Akke M (2006a) Biosynthetic 13C labeling of aromatic side-chains in proteins for NMR relaxation measurements. J Am Chem Soc 128:2506–2507

Teilum K, Poulsen FM, Akke M (2006b) The inverted chevron plot measured by NMR relaxation reveals a native-like unfolding intermediate in acyl-coA binding protein. Proc Natl Acad Sci USA 103:6877–6882

Vallurupalli P, Hansen DF, Stollar E, Meirovitch E, Kay LE (2007) Measurement of bond vector orientations in invisible excited states of proteins. Procm Natl Acad Sci USA 104:18473–18477

van Ingen H, Korzhnev DM, Kay LE (2009) An analysis of the effects of $^{1}H^{N}$-$^{1}H^{N}$ dipolar couplings on the measurement of amide bond vector orientations in invisible protein states by relaxation dispersion NMR. J Phys Chem B 113:9968–9977

Veeman WS (1984) Carbon-13 chemical shift anisotropy. Prog NMR Spectrosc 16:193–235

Weininger U, Diehl C, Akke M (2012) 13C relaxation experiments for aromatic side chains by longitudinal- and transverse-relaxation optimized NMR spectroscopy. J Biomol NMR. doi: 10.1007/s10858-012-9650-5

Wüthrich K, Wagner G (1975) NMR investigations of the dynamics of the aromatic amino acid residues in the basic pancreatic trypsin inhibitor. FEBS Lett 50:265–268

Zeeb M, Balbach J (2005) NMR spectroscopic characterization of millisecond protein folding by transverse relaxation dispersion measurements. J Am Chem Soc 127:13207–13212